Influence of the sampling time on the kinematics of turbulent diffusion from a continuous source

By RICHARD M. ECKMAN

Atmospheric Turbulence and Diffusion Division, NOAA/ARL, Oak Ridge, TN 37831, USA

A kinematic description is presented of how turbulent diffusion from a continuous source varies with the sampling time in stationary, homogeneous turbulence. Unlike most previous theories, the sampling is assumed to take place at fixed downstream distances from the source. It is shown that the sampling-time effects depend on two-particle velocity statistics. Thus, time-average diffusion at fixed downstream distances is more akin to relative diffusion than to absolute diffusion. Two simple diffusion models are developed from the kinematic equations. These models are in fairly good agreement with diffusion data obtained both in a wind tunnel and in the field. Moreover, these models have significant practical implications. For example, the models indicate that care must be taken when using band-pass spectral filtering as a paradigm for turbulent diffusion. Also, the models show that the mean flow speed U has an important influence on the sampling-time effects. To account for U properly, diffusion measurements with differing sampling times Λ should be compared using the product $U\Lambda$, and not just Λ.

1. Introduction

Statistical theories of turbulent diffusion such as Taylor's (1921) equation can describe only the ensemble-average characteristics of contaminant clouds. Ideally, any measurements of turbulent diffusion that are used to test these theories should also represent ensemble averages over many realizations of the turbulence field. In practice, however, ensemble-average diffusion measurements are often difficult to obtain, so the theories are instead compared with time-average measurements taken at fixed downstream distances from a continuous source. Time averaging is especially prevalent in atmospheric field measurements of plume concentration, since it is rarely possible to observe a large number of identical realizations of atmospheric turbulence. The time interval over which the concentration is sampled and averaged, called the sampling time, typically ranges from a few minutes to an hour in atmospheric field experiments (Wollenweber & Panofsky 1989).

As the sampling time increases, measured plume concentration distributions tend to widen. The reason for this behaviour is that time averaging suppresses the contributions of turbulent eddies having characteristic timescales significantly larger than the sampling time. Increasing the sampling time thus allows a progressively larger range of eddy sizes to influence the diffusion.

The well-known kinematic theories of turbulent diffusion are valid only at either asymptotically large or asymptotically small sampling times. Taylor's (1921) equation, for example, describes the ensemble-average diffusion of a single marked fluid particle. If ergodicity is assumed, Taylor's equation also represents time-average plume diffusion when the sampling time is asymptotically large; this is the so-called absolute

diffusion of the plume. Diffusion in the opposite limit of small sampling times corresponds to the plume's relative diffusion, as described by Richardson (1926) and Batchelor (1952). Other diffusion theories and models are also generally restricted to either absolute or relative diffusion (e.g. Sutton 1953; Smith & Hay 1961; Batchelor 1964; Thompson 1987).

Ogura (1957, 1959) was one of the first to develop a diffusion theory that explicitly includes the sampling time. His theory has been the focus for most of the subsequent discussions of the sampling time, such as Hino (1968), Doran, Horst & Nickola (1978), and Sheih (1980). Pasquill & Smith (1983) and Eckman (1989) have indicated, however, that Ogura's theory is obtained by sampling the turbulent motion of a single fluid particle over a finite time interval. This single-particle sampling is quite different from the type of sampling that is employed in practice, in which the plume concentration is sampled over a finite interval at fixed downstream distances from the source. There is no reason to believe that these two types of sampling are kinematically equivalent. For example, the mean flow speed U has no direct effect on the single-particle sampling used in Ogura's theory, because the sampling is purely Lagrangian in nature. In contrast, U has a significant effect on the time-average diffusion at a fixed downstream distance from the source, since a change in U will alter the frequency distribution of the turbulence at a fixed point.

In this paper, kinematic equations are developed to describe the effects of the sampling time on turbulent diffusion from a continuous source. The sampling is assumed to take place at fixed downstream distances from the source, as is the usual practice in the measurement of turbulent diffusion. For simplicity and tractability, the discussion is restricted to stationary, homogeneous turbulence. It is shown how the sampling-time effects depend on two-particle velocity statistics. The kinematic equations are then used to derive simpler diffusion models involving Eulerian velocity spectra. Finally, these models are compared with diffusion measurements taken in a wind tunnel and over flat terrain in Denmark.

2. Basic concepts

Consider a continuous source of marked fluid located in a turbulent flow with a constant mean flow speed U. The turbulence is assumed to be stationary and homogeneous. A coordinate system is oriented in this turbulence field so that the x_1 component of a position vector x is in the downstream direction, whereas the x_2 and x_3 components are in cross-stream directions. The source strength $S(x\,t)$ at time t describes the quantity of marked fluid released per unit volume and unit time. For simplicity, it is assumed that the centre of the source is at $x = 0$ at all t:

$$\int x_n \, S(x, t) \, \mathrm{d}x = 0. \tag{1}$$

The volume integral extends over the entire region occupied by the turbulent flow, and $n = 1, 2, 3$. Unless stated otherwise, spatial integrals in this paper are assumed to extend over all possible coordinate positions.

If $c(x, t)$ denotes the concentration of marked fluid at a point in space and time, then the absolute diffusion of the continuous plume is described by the ensemble-average concentration $\langle c(x, t) \rangle$. Angular brackets are used throughout this paper to denote

ensemble averaging. The ensemble-average concentration is related to the source strength by the equation (Monin & Yaglom 1971, §10)

$$\langle c(x, t)\rangle = \int_{s \leqslant t} ds \int S(x_0, s) Q(x - x_0 | t - s) dx_0. \tag{2}$$

Here, $Q(x - x_0 | t - s)$ is the probability density function for the displacement $x - x_0$ of a single fluid particle over a travel time $t - s$ in homogeneous, stationary turbulence.

The most useful aspects of the distribution $\langle c(x, t)\rangle$ are its second moments in the cross-stream directions. Given (1), these moments are defined as

$$D_{ij}(x_1, t) = \frac{\int dx_2 \int x_i x_j \langle c(x, t)\rangle dx_3}{\int dx_2 \int \langle c(x, t)\rangle dx_3}, \tag{3}$$

where $i, j = 2, 3$. Taylor's (1921) equation can be used to estimate the absolute-diffusion tensor D_{ij} if the travel time T of the marked fluid reaching x_1 is assumed to equal x_1/U (e.g. Monin & Yaglom 1971, §10; Kristensen, Jensen & Petersen 1981).

Relative diffusion deals with the distribution of marked fluid about the plume's instantaneous centreline, so it is associated with the ensemble-average covariance $\langle c(x, t) c(x + \Delta, t)\rangle$. This covariance is related to the source distribution by the integral (Durbin 1980; Thomson 1990)

$$\langle c(x, t) c(x + \Delta, t)\rangle = \int_{s' \leqslant t} ds' \int_{s'' \leqslant t} ds'' \int dx_0 \int S(x_0, s') S(x_0 + \Delta_0, s'')$$
$$\times q(x - x_0, \Delta | \Delta_0, s'' - s', t - s', t - s'') d\Delta_0. \tag{4}$$

The function $q(x - x_0, \Delta | \Delta_0, s'' - s', t - s', t - s'')$ is the joint probability density function for the displacement $x - x_0$ and separation Δ of two marked fluid particles. One particle is released at (x_0, s') and reaches the point x at time t. The second particle is released at $(x_0 + \Delta_0, s'')$ and is separated from the first particle by Δ at time t. The functional form of q given in (4) applies only to stationary and homogeneous turbulence. Although the three times that appear in q are not independent, they are retained here for consistency with the derivations in §3.

As with absolute diffusion, the most useful aspects of relative diffusion are second-order tensors in the cross-stream directions:

$$d_{ij}(x_1, t) = \frac{\int dx_2 \int dx_3 \int d\Delta_2 \int \Delta_i \Delta_j \langle c(x, t) c(x + \Delta, t)\rangle d\Delta_3}{\int dx_2 \int dx_3 \int d\Delta_2 \int \langle c(x, t) c(x + \Delta, t)\rangle d\Delta_3}. \tag{5}$$

The downstream component Δ_1 of the separation is set equal to zero in this equation. If the travel time T of the particles reaching x_1 is equal to x_1/U, Batchelor's (1952) theory for relative diffusion can be used to estimate d_{ij}. A number of researchers, including Smith & Hay (1961), Mikkelsen, Larsen & Pécseli (1987), and Georgopoulos & Seinfeld (1988), have developed simplified models for the variation of the relative-diffusion tensor with the travel time or downstream distance.

3. Kinematics of time-average diffusion

Although the theory developed by Ogura (1957) uses a single-particle sampling procedure that is quite different from that employed in practice, it has still been widely

used to estimate time-average diffusion (e.g. Hino 1968; Doran *et al.* 1978; Pasquill & Smith 1983) because of its simplicity and close association with Taylor's (1921) equation. Relatively little effort has been made to develop a kinematic diffusion model that accounts for finite sampling at fixed downstream distances.

Shimanuki (1961) recognized that a more realistic theory for the sampling time requires the consideration of marked fluid particles having different release times. He developed a kinematic equation for the time-average diffusion of a streak line (i.e. the plume from a continuous point source). However, the restriction of his equation to streak lines leads to unrealistic results at small sampling times. In addition, Shimanuki did not explicitly consider the dependence of streak-line diffusion on two-particle velocity statistics.

Monin & Yaglom (1975, §24) and Kristensen *et al.* (1981) also discussed the time-average diffusion of streak lines. Monin & Yaglom's discussion is very brief and closely parallels Shimanuki's (1961) work. Kristensen *et al.* independently derived equations for streak-like diffusion in their discussion of plume meandering in a stable atmosphere. They went on to develop a simple model for streak-line diffusion that includes both Eulerian and Lagrangian velocity correlations. Since the discussions of the sampling time by Shimanuki (1961), Monin & Yaglom (1975), and Kristensen *et al.* (1981) are restricted to streak lines and are rather limited, the kinematic effects of the sampling time are considered in more detail in this section.

Before proceeding with the mathematical derivations, it should be noted that the inclusion of time averages in a statistical diffusion model does not eliminate the need for ensemble averages. Unless the sampling time is asymptotically large, an ergodic hypothesis cannot be used to replace ensemble averages with time averages. Hence, the derivations given in this section contain both time and ensemble averages.

One can first consider the effects of time averaging on the absolute diffusion of a plume. Since the absolute diffusion is described by the ensemble-average concentration $\langle c(x, t) \rangle$, the effects of time averaging at the fixed point x are given by the integral

$$C(x, t, \Lambda) = \frac{1}{\Lambda} \int_{t-\Lambda/2}^{t+\Lambda/2} \langle c(x, r) \rangle \, \mathrm{d}r. \tag{6}$$

The variable Λ is the sampling time. Clearly, the time-average concentration $C(x, t, \Lambda)$ will differ from $\langle c(x, r) \rangle$ when the source strength varies with time. However, when the source strength is constant with time and the turbulence is stationary, $\langle c(x, r) \rangle$ is no longer a function of r, so $C(x, t, \Lambda)$ will equal $\langle c(x, r) \rangle$. Hence, the sampling time Λ only plays a role for absolute diffusion in stationary turbulence when the source strength varies with time.

Since measured concentration distributions tend to widen with the sampling time even when the source strength is constant, the widening must not be an absolute-diffusion phenomenon. It must therefore be more closely linked to relative diffusion. The reason for this linkage is that plume concentration distributions are usually measured with respect to the time-average plume centreline, and not with respect to a fixed coordinate origin.

To describe the diffusion of the plume about the time-average centreline, it is necessary to consider the ensemble-average covariance $\langle c(x, t') c(x+\Delta, t'') \rangle$. This is similar to the relative-diffusion covariance used in §2, except for the appearance of two times t' and t''. A linkage of this covariance to the source strength $S(x, t)$ can be made through the equation (Thomson 1990)

$$\langle c(x,t')\,c(x+\varDelta,t'')\rangle = \int_{s'\leqslant t'}\mathrm{d}s' \int_{s''\leqslant t''}\mathrm{d}s'' \int \mathrm{d}x_0 \int S(x_0,s')\,S(x_0+\varDelta_0,s'')$$
$$\times q(x-x_0,\varDelta\,|\,\varDelta_0, s''-s', t'-s', t''-s'')\,\mathrm{d}\varDelta_0. \quad (7)$$

The joint probability density function q has already been defined in §2.

The most important aspects of $\langle c(x,t')\,c(x+\varDelta,t'')\rangle$ from a practical viewpoint are its variability with $\varDelta_2$ and $\varDelta_3$ at a fixed downstream distance x_1. Thus, it is useful to define the function

$$P(\varDelta_2,\varDelta_3\,|\,x_1,t',t'') = \frac{\displaystyle\int \mathrm{d}x_2 \int \langle c(x,t')\,c(x+\varDelta,t'')\rangle\,\mathrm{d}x_3}{\displaystyle\int \mathrm{d}x_2 \int \mathrm{d}x_3 \int \mathrm{d}\varDelta_2 \int \langle c(x,t')\,c(x+\varDelta,t'')\rangle\,\mathrm{d}\varDelta_3}, \quad (8)$$

where $\varDelta_1$ is set equal to zero. This can be interpreted as the joint probability density function for finding two marked fluid particles separated by $(\varDelta_2,\varDelta_3)$ at a downstream distance x_1 from a continuous source, given that one of the particles reaches x_1 at time t' and the other reaches this downstream distance at t''.

The effects on the plume diffusion of sampling the concentration over an interval $\varLambda$ are obtained by averaging $P(\varDelta_2,\varDelta_3\,|\,x_1,t',t'')$ over both t' and t'':

$$\overline{P_\varLambda}(\varDelta_2,\varDelta_3\,|\,x_1,t) = \frac{1}{\varLambda^2}\int_{t-\frac{1}{2}\varLambda}^{t+\frac{1}{2}\varLambda}\mathrm{d}t' \int_{t-\frac{1}{2}\varLambda}^{t+\frac{1}{2}\varLambda} P(\varDelta_2,\varDelta_3\,|\,x_1,t',t'')\,\mathrm{d}t''. \quad (9)$$

As with the relative diffusion described in §2, the most useful aspects of this time-average function are the second moments

$$\varSigma_{ij}(x_1;t,\varLambda) = \int \mathrm{d}\varDelta_2 \int \varDelta_i\,\varDelta_j\,\overline{P_\varLambda}(\varDelta_2,\varDelta_3\,|\,x_1,t)\,\mathrm{d}\varDelta_3, \quad (10)$$

where $i,j = 2,3$. The square root of this tensor $\varSigma_{ij}$ can be interpreted as the 'width' of the time-average plume at the downstream distance x_1.

The general description of time-average diffusion as given by equations (7)–(10) is a highly complex two-particle diffusion process. To proceed further it is necessary to make some simplifying assumptions. First, it is assumed that the source strength is constant with time, so that $S(x,t) = S(x)$. Secondly, it is assumed that the travel times of the marked fluid particles reaching the downstream distance x_1 are narrowly distributed about the value x_1/U (Monin & Yaglom 1971, §10; Kristensen *et al.* 1981). This latter assumption is commonly invoked in plume diffusion modelling and is reasonable if two conditions are fulfilled. First, the turbulent velocity fluctuations in the downstream direction must be small compared to U so that the streamwise diffusion can be neglected (see Kristensen *et al.* 1981). Secondly, the 'length' of the source distribution $S(x)$ in the downstream direction must be small compared with x_1. This restriction on the source ensures that all the marked particles reaching x_1 have been advected nearly the same distance by the mean flow speed U.

One major effect of these simplifying assumptions is that the probability density function $P(\varDelta_2,\varDelta_3\,|\,x_1,t',t'')$ is determined only by the marked fluid released from the source at the two instants $t'-T$ and $t''-T$, where $T = x_1/U$. In other words, this function can be estimated by considering two instantaneous puffs that are sequentially
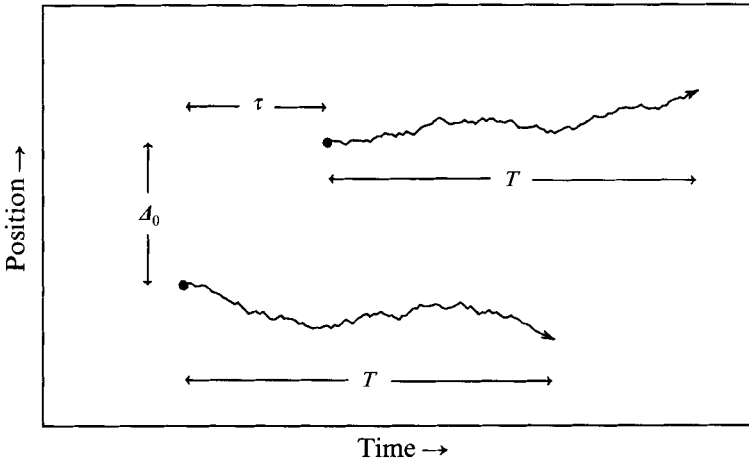
FIGURE 1. Schematic illustration of two fluid particles having release positions separated by Δ_0 and release times separated by $\tau = t'' - t'$. Both particles travel a time T before the final separation Δ is observed. For simplicity, the particle separation is shown only in one dimension.

released from the source at times separated by $t'' - t'$. The source strength of each puff, when normalized by the total mass of the puff, is

$$N(x) = \frac{S(x)}{\int S(x)\,dx}, \tag{11}$$

and the distribution $I(\Delta_0)$ of particle-pair separations at the source is defined as

$$I(\Delta_0) = \int N(x)\,N(x + \Delta_0)\,dx. \tag{12}$$

Given the simplifying assumptions discussed above, the function $P(\Delta_2, \Delta_3 \,|\, x_1, t', t'')$ is related to the distribution $I(\Delta_0)$ through the integral

$$P(\Delta_2, \Delta_3 \,|\, x_1, t', t'') = \int q(\Delta_2, \Delta_3 \,|\, \Delta_0, t'' - t', T)\,I(\Delta_0)\,d\Delta_0. \tag{13}$$

Here, $q(\Delta_2, \Delta_3 \,|\, \Delta_0, t'' - t', T)$ is the joint probability density function for the cross-stream separation (Δ_2, Δ_3) at travel time T of two marked fluid particles. These particles are released at times separated by $t'' - t'$ and from positions separated by Δ_0. Figure 1 is a schematic illustration of the two particles.

The right-hand side of (13) shows that $P(\Delta_2, \Delta_3 \,|\, x_1, t', t'')$ is a function of the difference $t'' - t'$, but not of each time separately. Hence, the time-average probability density function $\overline{P_A}(\Delta_2, \Delta_3 \,|\, x_1, t)$ is given by

$$\overline{P_A}(\Delta_2, \Delta_3 \,|\, x_1, t) = \frac{1}{A} \int_{-A}^{A} d\tau \int \left[1 - \frac{|\tau|}{A}\right] q(\Delta_2, \Delta_3 \,|\, \Delta_0, \tau, T)\,I(\Delta_0)\,d\Delta_0, \tag{14}$$

where $\tau = t'' - t'$ is the difference in release times. In addition, the time-average diffusion tensor Σ_{ij} defined by (10) becomes

$$\Sigma_{ij}(T; A) = \frac{1}{A} \int_{-A}^{A} d\tau \int d\Delta_0 \int d\Delta_2 \int \left[1 - \frac{|\tau|}{A}\right] \Delta_i \Delta_j\, q(\Delta_2, \Delta_3 \,|\, \Delta_0, \tau, T)\,I(\Delta_0)\,d\Delta_3. \tag{15}$$

Note that the dependence of Σ_{ij} in t has been eliminated, and the dependence on x_1 has been replaced by a dependence on $T = x_1/U$. If the tensor

$$\psi_{ij}(T;\varDelta_0,\tau) = \int \mathrm{d}\varDelta_2 \int \varDelta_i \varDelta_j q(\varDelta_2,\varDelta_3 \mid \varDelta_0,\tau,T)\,\mathrm{d}\varDelta_3 \tag{16}$$

represents the relative diffusion of two fluid particles having release points separated by $\varDelta_0$ and release times separated by τ, equation (15) can be further reduced to

$$\Sigma_{ij}(T;\varLambda) = \frac{1}{\varLambda}\int_{-\varLambda}^{\varLambda} \mathrm{d}\tau \int \left[\left[1 - \frac{|\tau|}{\varLambda}\right]\psi_{ij}(T;\varDelta_0,\tau)\,I(\varDelta_0)\,\mathrm{d}\varDelta_0. \tag{17}$$

Equation (17) shows that the time-average diffusion tensor Σ_{ij} for a plume is obtained by averaging the two-particle tensor ψ_{ij} over a temporal window determined by the sampling time $\varLambda$ and over a spatial window determined by the source distribution. An important implication of this result is that the sampling-time effects that are experimentally observed actually correspond to a form of two-particle diffusion, and not to single-particle diffusion. This contrasts with the single-particle nature of Ogura's (1957) equation for time-average diffusion.

The two-particle diffusion ψ_{ij} defined by (16) differs from that which is normally considered (e.g. Batchelor 1952) because of the release-time lag τ. If Taylor's frozen-eddy hypothesis is assumed to be valid, this lag adds an extra separation of $-U\tau$ between the two particles, where $U = (U,0,0)$ is the mean velocity vector. The tensor ψ_{ij} can then be interpreted as the relative diffusion of two marked particles that are simultaneously released with an initial separation $\varDelta_0 - U\tau$, although this interpretation is complicated by the two particles having different travel times.

4. Two-particle diffusion with a release-time lag

The derivation in the previous section showed that the time-average diffusion from a continuous source with constant output is determined by the source configuration $I(\varDelta_0)$ and by the two-particle diffusion tensor $\psi_{ij}(T;\varDelta_0,\tau)$. The dependence of ψ_{ij} on the turbulence structure is considered in this section.

4.1. *Relation to the turbulent velocity field*

An equation for ψ_{ij} can be developed by considering the position and velocities of two marked fluid particles as a function of the travel time T. The first particle is released at some (arbitrary) space–time position (x_0,t_0). Its position vector and velocity after travel time T have cross-stream components respectively denoted by $X_i(T;x_0,t_0)$ and $u_i(T;x_0,t_0)$ ($i = 2,3$). The second particle is released at $(x_0+\varDelta_0,t_0+\tau)$ and has later positions and velocities given by $X_i(T;x_0+\varDelta_0,t_0+\tau)$ and $u_i(T;x_0+\varDelta_0,t_0+\tau)$.

The tensor ψ_{ij} is related to the separation

$$\xi_i(T;x_0,\varDelta_0,t_0,\tau) = X_i(T;x_0+\varDelta_0,t_0+\tau) - X_i(T;x_0,t_0) \tag{18}$$

between the particles. Note that this separation is determined when the travel times of the particles are equal; the observation times t_0+T and $t_0+\tau+T$ of the particles are different. The separation ξ_i is related to the relative velocity

$$v_i(T;x_0,\varDelta_0,t_0,\tau) = u_i(T;x_0+\varDelta_0,t_0+\tau) - u_i(T;x_0,t_0) \tag{19}$$

through the equations

$$\xi_i(T;x_0,\varDelta_0,t_0,\tau) = \xi_i(0;x_0,\varDelta_0,t_0,\tau) + \int_0^T v_i(r;x_0,\varDelta_0,t_0,\tau)\,\mathrm{d}r, \tag{20}$$

$$v_i(T;x_0,\varDelta_0,t_0,\tau) = \frac{\partial}{\partial T}\xi_i(T;x_0,\varDelta_0,t_0,\tau). \tag{21}$$

For simplicity, the notations $\xi_i(T; x_0, \varDelta_0, t_0, \tau)$ and $v_i(T; x_0, \varDelta_0, t_0, \tau)$ are reduced to $\xi_i(T)$ and $v_i(T)$ in the following discussion.

An expression for $\psi_{ij}(T; \varDelta_0, \tau)$ is obtained from (20) and (21) by following the same procedure as used in the derivation of Taylor's (1921) equation. First, the equations are combined to obtain an expression for the product $\xi_i \xi_j$:

$$\frac{\partial \xi_i \xi_j}{\partial T} = \xi_i(0) v_j(T) + \xi_j(0) v_i(T) + \int_0^T [v_i(T) v_j(r) + v_j(T) v_i(r)] \, dr. \tag{22}$$

Secondly, ensemble averaging is performed on each side of (22) to obtain an expression for $\psi_{ij} = \langle \xi_i \xi_j \rangle$:

$$\frac{\partial \langle \xi_i \xi_j \rangle}{\partial T} = \frac{\partial \psi_{ij}}{\partial T} = \int_0^T [\langle v_i(T) v_j(r) \rangle + \langle v_j(T) v_i(r) \rangle] \, dr$$

$$= \int_0^T [R_{ij}(T, r; \varDelta_0, \tau) + R_{ji}(T, r; \varDelta_0, \tau)] \, dr. \tag{23}$$

The function $R_{ij}(T, r; \varDelta_0, \tau)$ is the autocovariance for the relative velocity v_i. This autocovariance is not stationary and thus depends on T and r separately. The first two terms on the right-hand side of (22) are not present in (23), because $\xi_i(0)$ is not a stochastic variable and $\langle v_i(T) \rangle = 0$.

Equation (23) has the same basic form as Taylor's (1921) formula for absolute diffusion and Batchelor's (1952) formula for relative diffusion; the left-hand side of the equation is the rate of change of the diffusion tensor, whereas the right-hand side is an integral over a velocity autocovariance. Unlike Taylor's and Batchelor's formulae, however, (23) involves particles released at two different times.

The general form of $R_{ij}(T, r; \varDelta_0, \tau)$ is unknown, so it is not possible to write a general solution to (23). However, the traditional near-field and far-field limits of Taylor's equation have their analogues in (23). The near-field limit occurs when T is small enough that $v_i(T)$ has changed little from its initial value $v_i(0)$. In this case, (23) can be written as

$$\frac{\partial \psi_{ij}}{\partial T} = T[R_{ij}(0, 0; \varDelta_0, \tau) + R_{ji}(0, 0; \varDelta_0, \tau)]. \tag{24}$$

Thus, ψ_{ij} is proportional to T^2 in the near-field limit.

The autocovariance $R_{ij}(0, 0, \varDelta_0, \tau)$ in (24) depends only on the initial velocities of the marked particles, so it provides a purely Eulerian description of the turbulence. An Eulerian space–time covariance $R_{ij}^E(\varDelta_0, \tau)$ for the turbulent velocity can be defined as

$$R_{ij}^E(\varDelta_0, \tau) = \langle u_i(0; x_0, t_0) u_j(0; x_0 + \varDelta_0, t_0 + \tau) \rangle, \tag{25}$$

where u_i was defined at the beginning of this section. This covariance describes the relation between the velocity fluctuations at two points separated by $\varDelta_0$ in space and τ in time. The autocovariance $R_{ij}(0, 0, \varDelta_0, \tau)$ is related to R_{ij}^E through the equation

$$R_{ij}(0, 0, \varDelta_0, \tau) = 2\eta_{ij} - R_{ij}^E(\varDelta_0, \tau) - R_{ji}^E(\varDelta_0, \tau). \tag{26}$$

Here, $\eta_{ij} = R_{ij}^E(0, 0)$ represents the velocity covariance when both the time and space lags are zero.

With (26), the near-field limit described by (24) becomes

$$\frac{\partial \psi_{ij}}{\partial T} = 2T[2\eta_{ij} - R_{ij}^E(\varDelta_0, \tau) - R_{ji}^E(\varDelta_0, \tau)]. \tag{27}$$

Moreover, if this limit is valid for all the time lags τ and initial separations Δ_0 that appear in (17), then the continuous-plume tensor Σ_{ij} is given by

$$\Sigma_{ij}(T;\Lambda) = \Sigma_{ij}(0;\Lambda) + T^2 \Big\{ 2\eta_{ij}$$

$$- \frac{1}{\Lambda} \int_{-\Lambda}^{\Lambda} \mathrm{d}\tau \int \Big(1 - \frac{|\tau|}{\Lambda}\Big) [R_{ij}^E(\Delta_0,\tau) + R_{ji}^E(\Delta_0,\tau)] \, I(\Delta_0) \, \mathrm{d}\Delta_0 \Big\}. \quad (28)$$

This equation shows that in the near field, the time-averaged diffusion of a continuous plume is obtained by averaging the Eulerian space–time covariance $R_{ij}^E(\Delta_0,\tau)$ over a spatial window weighted by the source configuration I and over a temporal window weighted by $1 - |\tau|/\Lambda$.

The far-field limit of (23) is reached when the velocity fluctuations u_i of the two fluid particles become uncorrelated. In this case, the autocorrelation $R_{ij}(T,r;\Delta_0,\tau)$ reduces to

$$R_{ij}(T,r;\Delta_0,\tau) = 2\langle u_i(T;x_0,t_0)\,u_j(r;x_0,t_0)\rangle$$

$$= 2R_{ij}^L(T-r). \quad (29)$$

Here, $R_{ij}^L(T-r)$ is the Lagrangian autocovariance. The travel time T at which this limit first becomes valid generally depends both on the Lagrangian timescale of the turbulence and on the initial separation of the two fluid particles.

When (29) is valid, (23) becomes

$$\frac{\partial \psi_{ij}}{\partial T} = 2 \int_0^\infty [R_{ij}^L(T-r) + R_{ji}^L(T-r)] \, \mathrm{d}r. \quad (30)$$

The left-hand side of this equation is a constant proportional to the Lagrangian timescale, so the tensor ψ_{ij} varies linearly with the travel time, a behaviour similar to Taylor's (1921) formula in the far-field limit. At sufficiently large travel times, (30) will apply to all the particle pairs in a plume, so the plume tensor Σ_{ij} also varies linearly in the far field.

4.2. *Diffusion in the inertial subrange*

Further information about ψ_{ij} in the inertial subrange can be obtained with Kolmogorov's similarity hypotheses, as was done by Batchelor (1950) for relative diffusion. For ψ_{ij}, however, the release-time lag τ makes application of the similarity hypotheses more difficult. During this time lag, the mean velocity U of the flow will advect the first fluid particle away from the source. Hence, U must be added to the list of parameters for which ψ_{ij} is a function. However, this problem can be avoided by changing from a fixed coordinate system to another inertial system that moves with the mean flow velocity U. In this new system, the release-time lag for the two particles is still τ, but the initial separation between the particles is $\Delta_0 - U\tau$, as shown in figure 2. Hence, the mean velocity appears only as an adjustment to the particles' initial separation in the moving coordinate system.

To apply the similarity hypotheses, it must be assumed that ψ_{ij} is affected only by turbulent eddies in the inertial or dissipation subranges. The diffusion then depends on the kinematic viscosity ν and the rate of dissipation ϵ of turbulent kinetic energy, in addition to T, τ, and $\Delta_0 - U\tau$. The general similarity expression for ψ_{ij} can be written as

$$\frac{\partial \psi_{ij}}{\partial T} = \epsilon T^2 G\Big(\frac{\nu}{\epsilon T^2}, \frac{|\Delta_0 - U\tau|}{\epsilon^{\frac{1}{2}} T^{\frac{3}{2}}}, \frac{\tau}{T}\Big), \quad (31)$$
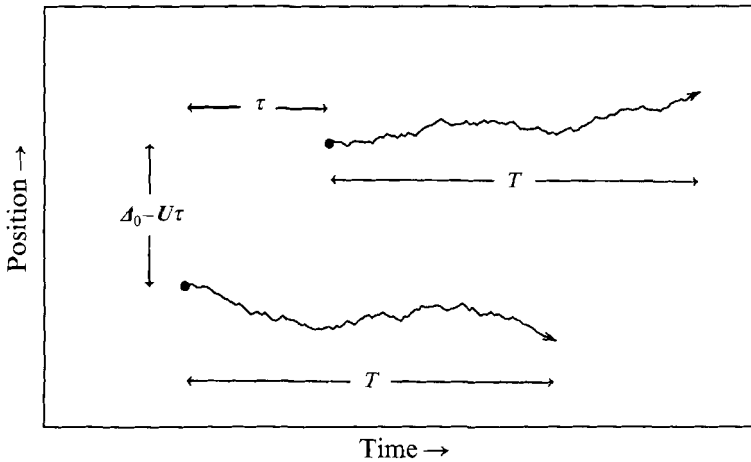
FIGURE 2. Diffusion of two fluid particles in a coordinate system moving with the mean flow velocity U. The particles' release positions are separated by $\varDelta_0 - U\tau$, and their release times are separated by τ. For simplicity, the particle separation is shown only in one dimension.

where $|\varDelta_0 - U\tau|$ is the magnitude of $\varDelta_0 - U\tau$, and G is a universal function. If the initial separation is within the inertial subrange, the viscosity can be ignored, and (31) simplifies to

$$\frac{\partial \psi_{ij}}{\partial T} = \epsilon T^2 G_1 \left(\frac{|\varDelta_0 - U\tau|}{\epsilon^{\frac{1}{2}} T^{\frac{3}{2}}}, \frac{\tau}{T} \right), \tag{32}$$

with G_1 being another universal function.

In the near-field limit, (24) applies. The similarity hypotheses in this limit can be applied to the velocity covariance $R_{ij}(0, 0; \varDelta_0, \tau)$, which depends on ν, ϵ, $|\varDelta_0 - U\tau|$, and τ. A similarity form of (24) is then

$$\frac{\partial \psi_{ij}}{\partial T} = T\epsilon^{\frac{2}{3}} |\varDelta_0 - U\tau|^{\frac{2}{3}} H \left(\frac{\nu}{\epsilon^{\frac{1}{3}} |\varDelta_0 - U\tau|^{\frac{4}{3}}}, \frac{\tau \epsilon^{\frac{1}{3}}}{|\varDelta_0 - U\tau|^{\frac{2}{3}}} \right). \tag{33}$$

H is a universal function. When $|\varDelta_0 - U\tau|$ is within the inertial subrange, H can be replaced by a simpler function H_1:

$$\frac{\partial \psi_{ij}}{\partial T} = T\epsilon^{\frac{2}{3}} |\varDelta_0 - U\tau|^{\frac{2}{3}} H_1 \left(\frac{\tau \epsilon^{\frac{1}{3}}}{|\varDelta_0 - U\tau|^{\frac{2}{3}}} \right). \tag{34}$$

If Taylor's frozen-eddy hypothesis is valid, the release-time lag τ affects the diffusion only by increasing the initial particle separation by $-U\tau$. The function H_1 in (34) thus represents the decay of the turbulent eddies that takes place over the interval τ. If this decay is small (i.e. the frozen-eddy hypothesis is valid) and $|\varDelta_0|$ is small compared with $|U\tau|$, equation (34) indicates that ψ_{ij} should be proportional to $|U\tau|^{\frac{2}{3}}$. Moreover, if $\psi_{ij} \propto |U\tau|^{\frac{2}{3}}$ is substituted into (17), then $\varSigma_{ij} \propto (U\varLambda)^{\frac{2}{3}}$. (This substitution is valid when $U\varLambda$ is significantly larger than the spatial dimensions of $I(\varDelta_0)$.) A similar $\frac{2}{3}$ power dependence for plume diffusion has previously been obtained by Hino (1968) and Pasquill & Smith (1983) using spectral arguments. However, (34) puts more restrictions on this result than the spectral derivations. First, it must be assumed that only turbulence within the inertial subrange affects the diffusion. Secondly, the diffusion must be in the near-field limit for which $\varSigma_{ij} \propto T^2$. Thirdly, Taylor's frozen-eddy hypothesis must be valid. Fourthly, the length $U\varLambda$ must be large compared with the initial size of the cloud.

Another important aspect of (34) is the effect of the mean flow speed U. If the eddy-decay function H_1 is neglected, a percentage change in U has the same effect on ψ_{ij} as an equivalent percentage change in τ. This equation therefore suggests that plume diffusion measurements with different sampling times should be compared based on the length $U\Lambda$ and not solely on the sampling time Λ. The effect of the mean flow speed is considered further in §5.

If the initial separation and release-time lag are sufficiently small, there may be a range of travel times for which ψ_{ij} only weakly depends on $\Lambda_0 - U\tau$ and τ but still has not reached the far-field limit in which the particles wander independently. This is similar to the intermediate range of travel times for relative diffusion discussed by Batchelor (1950). In this intermediate range, the universal function G_1 becomes a constant g_1, and the diffusion is described by

$$\frac{\partial \psi_{ij}}{\partial T} = g_1 \epsilon T^2. \tag{35}$$

The tensor ψ_{ij} is therefore proportional to T^3 in this range.

The travel time T_1 representing the transition from the near-field limit of (34) to the intermediate range of (35) follows a relation of the form

$$T_1 = \frac{|\Lambda_0 - U\tau|^{\frac{2}{3}}}{\epsilon^{\frac{1}{3}}} L\left(\frac{\tau \epsilon^{\frac{1}{3}}}{|\Lambda_0 - U\tau|^{\frac{2}{3}}}\right), \tag{36}$$

where L is another universal function. Like the function H_1 in (34), the function L represents the decay of the turbulent eddies over the period τ. If this decay is neglected, the transition time T_1 should be proportional to $|U\tau|^{\frac{2}{3}}$ provided $|\Lambda_0| \ll |U\tau|$.

Overall, the discussions in §4.1 and this section indicate that the three stages of growth discussed by Batchelor (1950) for relative diffusion can also be applied to the time-average diffusion Σ_{ij} of a continuous plume. In the near field, Σ_{ij} is proportional to T^2. At intermediate travel times, (35) indicates that Σ_{ij} may be proportional to T^3 if the inertial subrange has a large extent. At large travel times, Σ_{ij} becomes proportional to T. Equation (36) suggests that as the sampling time increases, the near-field range of travel times grows at the expense of the intermediate travel times. At sufficiently large sampling times, the intermediate range is completely eliminated, and Σ_{ij} reduces to the absolute diffusion described by Taylor's equation.

5. Simple models for the sampling time

The complexity of the equations derived in §§3 and 4 makes it difficult to relate the sampling-time effects to simple turbulence parameters. A general description of the time-average diffusion would in fact require detailed knowledge of the two-particle velocity covariance $R_{ij}(T, r; \Lambda_0, \tau)$ that appears in (23). In this section, two simple models are developed using assumptions similar to those employed by Sawford (1982) and Mikkelsen *et al.* (1987) for relative diffusion. Both of these papers use an assumption – originally proposed by G. I. Taylor in an unpublished 1935 note – that two-particle velocity covariances can be approximated as the product of purely Lagrangian and Eulerian velocity correlations. The relative diffusion considered by Sawford and Mikkelsen *et al.*, for example, is a function of the two-particle covariance $\langle u_i(T; x_0, t_0) u_j(r; x_0 + \Lambda_0, t_0) \rangle$. With Taylor's proposal, this can be approximated as

$$\langle u_i(T; x_0, t_0) u_j(r; x_0 + \Lambda_0, t_0) \rangle = \rho_{ij}^L(T-r) \int R_{ij}^E(\Lambda, 0) q(\Lambda \mid \Lambda_0, T) \, d\Lambda, \tag{37}$$

where $\rho_{ij}^L(T-r) = R_{ij}^L(T-r)/\eta_{ij}$, R_{ij}^E is defined by (25), and $q(\varDelta \,|\, \varDelta_0, T)$ is the probability density distribution for the separation at travel time T of two fluid particles simultaneously released with an initial separation $\varDelta_0$.

The effect of (37) on the kinematics of relative diffusion can be obtained from (17) and (23) by setting $\varLambda$ (and thus τ) equal to zero. First, (37) is used in (23) to provide a modified equation for ψ_{ij}; this equation for ψ_{ij} is then used in (17) to obtain an expression for the relative-diffusion tensor $\varSigma_{ij}(T;0)$. The resulting equation is

$$\frac{\partial \varSigma_{ij}(T;0)}{\partial T} = \left\{ \int_0^T [\rho_{ij}^L(T-r) + \rho_{ji}^L(T-r)]\,\mathrm{d}r \right\}$$

$$\times \left\{ 2\eta_{ij} - \int [R_{ij}^E(\varDelta,0) + R_{ji}^E(\varDelta,0)]\, I_T(\varDelta)\,\mathrm{d}\varDelta \right\}, \quad (38)$$

where
$$I_T(\varDelta) = \int q(\varDelta \,|\, T, \varDelta_0)\, I(\varDelta_0)\,\mathrm{d}\varDelta_0. \quad (39)$$

The function I_T represents the distribution of marked-particle separations at travel time T.

An interesting feature of (38) is that it closely resembles the near-field relative diffusion limit, which from (28) is given by

$$\frac{\partial \varSigma_{ij}(T;0)}{\partial T} = 2T \left\{ 2\eta_{ij} - \int [R_{ij}^E(\varDelta_0,0) + R_{ji}^E(\varDelta_0,0)]\, I(\varDelta_0)\,\mathrm{d}\varDelta_0 \right\}. \quad (40)$$

The only differences between (38) and (40) are the replacement of $I(\varDelta_0)$ with $I_T(\varDelta)$ and the replacement of $2T$ with an integral over ρ_{ij}^L. Aside from the integral over ρ_{ij}^L, equation (38) can therefore be interpreted as the rate of diffusion that would result if the diffusion is a Markov process that restarts at each travel time T.

The integral over ρ_{ij}^L that appears in (38) is a timescale that approaches $2T$ for small T and is proportional to the Lagrangian timescale of the turbulence for large T. Equation (38) can hence be expressed in the simple form

$$\frac{\partial \varSigma_{ij}(T;0)}{\partial T} = A_{ij}(T) \left[\frac{1}{2T}\frac{\partial \varSigma_{ij}}{\partial T} \right]_{Markov}, \quad (41)$$

in which
$$A_{ij}(T) = \int_0^T [\rho_{ij}^L(T-r) + \rho_{ji}^L(T-r)]\,\mathrm{d}r, \quad (42)$$

and the notation $[\;]_{Markov}$ is used to indicate that this term is obtained by restarting the diffusion at each travel time T using $I_T(\varDelta)$ as the initial source distribution.

Although (37) may not be valid in all circumstances, the work by Sawford (1982) and Mikkelsen (1987) indicates that (41) provides reasonable practical estimates of relative diffusion. A similar approach may thus be useful for providing practical estimates of the time-average diffusion. In the two following sections, simple models for the time-average diffusion are obtained by generalizing (41) for $\varLambda \neq 0$:

$$\frac{\partial \varSigma_{ij}(T;\varLambda)}{\partial T} = A_{ij}(T) \left[\frac{1}{2T}\frac{\partial \varSigma_{ij}}{\partial T} \right]_{Markov}. \quad (43)$$

These models provide some insight into how the sampling time affects $\varSigma_{ij}$ and how plume sampling at a fixed downstream distance differs from the single-particle sampling used in Ogura's (1957) equation.

5.1. *Continuous point source*

The first case to be considered is time-average diffusion from a continuous point source (i.e. a streak line). The initial distribution $I(\Delta_0)$ for a point source is equal to a delta function at $\Delta_0 = 0$. Thus, in the near-field limit the time-average diffusion of a streak line is from (28) given by

$$\frac{1}{2T}\frac{\partial \Sigma_{ij}(T;\Delta)}{\partial T} = 2\eta_{ij} - \frac{1}{\Delta}\int_{-\Delta}^{\Delta}\left(1 - \frac{|\tau|}{\Delta}\right)[R_{ij}^E(0,\tau) + R_{ji}^E(0,\tau)]\,d\tau. \tag{44}$$

If the Eulerian cospectrum $C_{ij}^E(\omega)$ at angular frequency ω is defined as

$$C_{ij}^E(\omega) = \frac{1}{2\pi}\int_{-\infty}^{\infty} R_{ij}^E(0,\tau)\cos(\omega\tau)\,d\tau, \tag{45}$$

then (44) reduces to

$$\frac{1}{2T}\frac{\partial \Sigma_{ij}(T;\Delta)}{\partial T} = 4\int_0^{\infty} C_{ij}^E(\omega)\left[1 - \frac{\sin^2(\tfrac{1}{2}\omega\Delta)}{(\tfrac{1}{2}\omega\Delta)^2}\right]d\omega. \tag{46}$$

One question that must be considered before applying (46) to (43) is how small does a real source need to be before it can be considered a point source. This question can be answered roughly by referring back to (28). As mentioned previously, Taylor's frozen-eddy hypothesis suggests that $R_{ij}^E(\Delta_0,\tau)$ can be estimated as the purely spatial covariance $R_{ij}^E(\Delta_0 - U\tau, 0)$. Equation (28) will then reduce to (44) if the condition $|U\tau| \gg |\Delta_0|$ is valid over most of the range $|\tau| \leqslant \Delta$, so that the contribution of the initial distribution $I(\Delta_0)$ is negligible. This condition will generally be valid when $U\Delta$ is much larger than the spatial dimensions of $I(\Delta_0)$. As a rough estimate, then, the source can be considered a point if its spatial dimensions are much smaller than $U\Delta$. The conditions for a source to be considered a point are considered further in §5.2.

To apply (46) to the Markov part of (43), it is necessary to assume that $U\Delta$ is significantly larger than the dimensions of the distribution $I_T(\Delta)$ at time T. The model for time-average diffusion from a point source then becomes

$$\frac{\partial \Sigma_{ij}(T;\Delta)}{\partial T} = 4A_{ij}(T)\int_0^{\infty} C_{ij}^E(\omega)\left[1 - \frac{\sin^2(\tfrac{1}{2}\omega\Delta)}{(\tfrac{1}{2}\omega\Delta)^2}\right]d\omega. \tag{47}$$

This can be further simplified by using the Lagrangian cospectrum

$$C_{ij}^L(\omega) = \frac{1}{2\pi}\int_{-\infty}^{\infty} R_{ij}^L(\tau)\cos(\omega\tau)\,d\tau \tag{48}$$

to write the timescale $A_{ij}(T)$ as

$$A_{ij}(T) = \frac{4}{\eta_{ij}}\int_0^{\infty} C_{ij}^L(\omega)\frac{\sin(\omega T)}{\omega}\,d\omega. \tag{49}$$

After integration over T, (47) then reduces to

$$\Sigma_{ij}(T;\Delta) = 8\frac{T^2}{\eta_{ij}}\int_0^{\infty} d\omega'\int_0^{\infty} C_{ij}^L(\omega')\,C_{ij}^E(\omega)\frac{\sin^2(\tfrac{1}{2}\omega'T)}{(\tfrac{1}{2}\omega'T)^2}\left[1 - \frac{\sin^2(\tfrac{1}{2}\omega\Delta)}{(\tfrac{1}{2}\omega\Delta)^2}\right]d\omega. \tag{50}$$

This equation is a spectral form of the streak-line model developed by Kristensen *et al.* (1981).

Equation (50) has some similarities to Ogura's (1957) equation, which can be written as (e.g. Eckman 1989)

$$D_{ij}(T;\Lambda) = 2T^2 \int_0^\infty C_{ij}^L(\omega) \frac{\sin^2\left(\frac{1}{2}\omega T\right)}{\left(\frac{1}{2}\omega T\right)^2} \left[1 - \frac{\sin^2\left(\frac{1}{2}\omega\Lambda\right)}{\left(\frac{1}{2}\omega\Lambda\right)^2}\right] d\omega. \tag{51}$$

The diffusion tensor is denoted by D_{ij} to indicate that it is a single-particle parameter related to the absolute-diffusion tensor described by (3).

The same filters are applied to the velocity spectra in both (50) and (51). However, there are important differences between the equations. First, only the Lagrangian cospectrum C_{ij}^L appears in (51), whereas both the Lagrangian and Eulerian cospectra appear in (50). Secondly, the high- and low-pass spectral filters in (51) combine to form a band-pass filter; this band-pass filtering is not found in (50), since the high- and low-pass filters apply to different frequency variables.

The band-pass filtering that appears in (51) has often been invoked (e.g. Hanna, Briggs & Hosker 1982; Panofsky & Dutton 1984; Georgopoulos & Seinfeld 1988) to explain various aspects of turbulent diffusion. However, this band-pass filtering is directly tied to the single-particle nature of Ogura's equation. Equation (50) indicates that such band-pass filtering does not occur when a more realistic sampling procedure is used for the diffusion. Thus, care must be taken when using band-pass filtering as a paradigm for turbulent diffusion.

Another important difference between (50) and (51) is the effect of the mean flow speed U. Variations in this flow speed affect the Eulerian cospectrum C_{ij}^E but not the Lagrangian cospectrum C_{ij}^L. This is easier to see if the frozen-eddy hypothesis is used to replace the Eulerian frequency cospectrum $C_{ij}^E(\omega)$ with the Eulerian wavenumber cospectrum $F_{ij}^E(k_1)$:

$$F_{ij}^E(k_1) = U C_{ij}^E(\omega), \tag{52}$$

where $k_1 = \omega/U$ is the wavenumber component in the downstream direction. Equation (50) can then be written as

$$\Sigma_{ij}(T,\Lambda) = 8\frac{T^2}{\eta_{ij}} \int_0^\infty d\omega' \int_0^\infty C_{ij}^L(\omega') F_{ij}^E(k_1) \frac{\sin^2\left(\frac{1}{2}\omega'T\right)}{\left(\frac{1}{2}\omega'T\right)^2} \left[1 - \frac{\sin^2\left(\frac{1}{2}k_1 U\Lambda\right)}{\left(\frac{1}{2}k_1 U\Lambda\right)^2}\right] dk_1. \tag{53}$$

Taylor's frozen-eddy hypothesis cannot be applied to (51), since $C_{ij}^L(\omega)$ is a Lagrangian cospectrum.

In (53), the speed U has a direct effect on the high-pass spectral filter: a larger value of U moves the cut-off of this filter towards lower wavenumbers. This is the speed dependence that one would expect when the plume sampling takes place at a fixed downstream distance from the source. No such speed dependence is found in (51). At first sight, Hay & Pasquill's (1959) suggested relation

$$C_{ij}^L(\omega) = \beta C_{ij}^E(\beta\omega) \tag{54}$$

between the Lagrangian and Eulerian frequency spectra may provide such a speed dependence. With this relation and (52), (51) can be reduced to

$$D_{ij}(T;\Lambda) = 2T^2 \int_0^\infty F_{ij}^E(k_1) \frac{\sin^2\left(k_1 UT/2\beta\right)}{\left(k_1 UT/2\beta\right)^2} \left[1 - \frac{\sin^2\left(k_1 U\Lambda/2\beta\right)}{\left(k_1 U\Lambda/2\beta\right)^2}\right] dk. \tag{55}$$

However, neither filter in this equation has a speed dependence, because the parameter β, which is the ratio of the Lagrangian to Eulerian timescales of the turbulence, is directly proportional to U (Pasquill & Smith 1983). Thus, the ratio U/β in (55) is constant with U.

5.2. *Gaussian source in inertial-subrange turbulence*

The second case to be considered here is the time-average diffusion from a symmetrical Gaussian source having a variance γ^2. The source distribution $I(\varDelta)$ of marked-particle separations is also Gaussian with a variance $2\gamma^2$:

$$I(\varDelta) = \frac{1}{8\pi^{\frac{3}{2}}\gamma^3}\exp\left(-\varDelta^2/4\gamma^2\right). \tag{56}$$

Here, $\varDelta$ is the magnitude of $\boldsymbol{\varDelta}$.

As in §5.1, the near-field diffusion limit given by (28) will be used as a starting point. Again, the Eulerian space–time covariance $R_{ij}^E(\varDelta_0, \tau)$ is assumed to be equal to the purely spatial covariance $R_{ij}^E(\varDelta_0 - U\tau, 0)$. Equation (28) can then be written as

$$\frac{1}{2T}\frac{\partial \Sigma_{ij}}{\partial T} = 2\eta_{ij} - \frac{1}{\varLambda}\int_{-\varLambda}^{\varLambda}\mathrm{d}\tau\int\left(1 - \frac{|\tau|}{\varLambda}\right)[R_{ij}^E(\varDelta_0 - U\tau, 0) + R_{ji}^E(\varDelta_0 - U\tau, 0)]\,I(\varDelta_0)\,\mathrm{d}\varDelta_0. \tag{57}$$

The energy spectrum tensor $\varPhi_{ij}(\boldsymbol{k})$ for a vector wavenumber $\boldsymbol{k}$ is the three-dimensional Fourier transform of the Eulerian velocity covariance $R_{ij}^E(\varDelta, 0)$ (see Batchelor 1953):

$$\varPhi_{ij}(\boldsymbol{k}) = \frac{1}{8\pi^3}\int R_{ij}^E(\varDelta, 0)\exp\left(-\mathrm{i}\boldsymbol{k}\cdot\varDelta\right)\mathrm{d}\varDelta, \tag{58}$$

$$R_{ij}^E(\varDelta, 0) = \int \varPhi_{ij}(\boldsymbol{k})\exp\left(\mathrm{i}\boldsymbol{k}\cdot\varDelta\right)\mathrm{d}\boldsymbol{k}. \tag{59}$$

The integral over $\boldsymbol{k}$ extends over all possible wavenumber coordinates. Equation (57) can now be expressed in the following spectral form:

$$\frac{1}{2T}\frac{\partial \Sigma_{ij}}{\partial T} = \int [\varPhi_{ij}(\boldsymbol{k}) + \varPhi_{ji}(\boldsymbol{k})]\left[1 - 8\pi^3 J^*(\boldsymbol{k})\frac{\sin^2\left(\frac{1}{2}k_1 U\varLambda\right)}{\left(\frac{1}{2}k_1 U\varLambda\right)^2}\right]\mathrm{d}\boldsymbol{k}. \tag{60}$$

The variable k_1 is the downstream component of $\boldsymbol{k}$, whereas $J(\boldsymbol{k})$ is the Fourier transform of $I(\varDelta)$:

$$J(\boldsymbol{k}) = \frac{1}{8\pi^3}\int I(\varDelta)\exp\left(-\mathrm{i}\boldsymbol{k}\cdot\varDelta\right)\mathrm{d}\varDelta. \tag{61}$$

The asterisk in (60) denotes a complex conjugate.

Equation (60) has some similarities to (50) in that the time-average diffusion is determined by windowing a velocity spectrum with a high-pass filter. However, in (60), the high-pass filter is affected by both the sampling time $\varLambda$ and the shape characteristics of the source (through J). For a Gaussian source described by (56), the Fourier transform J is

$$J(\boldsymbol{k}) = \frac{1}{8\pi^3}\exp\left(-k^2\gamma^2\right), \tag{62}$$

where k is the magnitude of $\boldsymbol{k}$. Hence, (60) for this Gaussian source becomes

$$\frac{1}{2T}\frac{\partial \Sigma_{ij}}{\partial T} = \int [\varPhi_{ij}(\boldsymbol{k}) + \varPhi_{ji}(\boldsymbol{k})]\left[1 - \exp\left(-k^2\gamma^2\right)\frac{\sin^2\left(\frac{1}{2}k_1 U\varLambda\right)}{\left(\frac{1}{2}k_1 U\varLambda\right)^2}\right]\mathrm{d}\boldsymbol{k}. \tag{63}$$

The function $\exp\left(-k^2\gamma^2\right)$ in (63) can be interpreted as a low-pass spectral filter having a cut-off at $k \approx 1/\gamma$, whereas $\sin^2\left(\frac{1}{2}k_1 U\varLambda\right)/\left(\frac{1}{2}k_1 U\varLambda\right)^2$ is a low-pass filter with a

cut-off at about $k_1 \approx 1/U\Lambda$. A high-pass spectral filter is created by subtracting the product of these two low-pass filters from unity. Equation (63) represents relative diffusion when $\Lambda < \gamma/U$, because the high-pass filtering is dominated by the function $\exp(-k^2\gamma^2)$ in this limit. Absolute diffusion is obtained when $U\Lambda$ is significantly larger than the characteristic lengthscale of the turbulence in the downstream direction.

Quantitative estimates of the time-average diffusion can be obtained from (63) by considering the simple case of isotropic turbulence. The functions Σ_{22} and Σ_{33} are equal in isotropic turbulence, so they can be replaced by the single function $2\sigma^2 = \Sigma_{22} = \Sigma_{33}$. The definition of σ conforms to the standard notation used in atmospheric diffusion to define the plume's half width. Since σ^2 can also be defined as $\frac{1}{4}(\Sigma_{22}+\Sigma_{33})$, (63) can be used to obtain

$$\frac{1}{T}\frac{\partial\sigma^2}{\partial T} = \int [\Phi_{22}(\mathbf{k})+\Phi_{33}(\mathbf{k})]\left[1-\exp(-k^2\gamma^2)\frac{\sin^2(\frac{1}{2}k_1 U\Lambda)}{(\frac{1}{2}k_1 U\Lambda)^2}\right]\mathrm{d}\mathbf{k}. \qquad (64)$$

In isotropic turbulence, the sum $\Phi_{22}(\mathbf{k})+\Phi_{33}(\mathbf{k})$ is given by (Batchelor 1953)

$$\Phi_{22}(\mathbf{k})+\Phi_{33}(\mathbf{k}) = \frac{E(k)}{4\pi k^4}(k^2+k_1^2), \qquad (65)$$

where $E(k)$ is the energy spectrum function. Equation (64) then becomes

$$\frac{1}{T}\frac{\partial\sigma^2}{\partial T} = \frac{1}{4\pi}\int E(k)\frac{k^2+k_1^2}{k^4}\left[1-\exp(-k^2\gamma^2)\frac{\sin^2(\frac{1}{2}k_1 U\Lambda)}{(\frac{1}{2}k_1 U\Lambda)^2}\right]\mathrm{d}\mathbf{k}. \qquad (66)$$

Through a conversion to spherical coordinates, this equation can be reduced to a single integral over the wavenumber magnitude k:

$$\frac{1}{T}\frac{\partial\sigma^2}{\partial T} = 2\int_0^\infty E(k)\left[\frac{2}{3}+\exp(-k^2\gamma^2)\frac{\sin(kU\Lambda)-(kU\Lambda)\cos(kU\Lambda)-(kU\Lambda)^2\,\mathrm{Si}(kU\Lambda)}{(kU\Lambda)^3}\right]\mathrm{d}k. \qquad (67)$$

The function $\mathrm{Si}(kU\Lambda)$ is the sine-integral function (Gautschi & Cahill 1964).

The near-field limit described by (67) can now be used as the Markov factor in (43). In this factor, the diffusion is restarted at travel time T using a Gaussian source with an initial variance equal to $\sigma^2(T;\Lambda)$:

$$\left[\frac{1}{T}\frac{\partial\sigma^2}{\partial T}\right]_{Markov} = \left[\frac{1}{2T}\frac{\partial\Sigma_{22}}{\partial T}\right]_{Markov}$$

$$= 2\int_0^\infty E(k)\left[\frac{2}{3}+\exp(-k^2\sigma^2)\frac{\sin(kU\Lambda)-(kU\Lambda)\cos(kU\Lambda)-(kU\Lambda)^2\,\mathrm{Si}(kU\Lambda)}{(kU\Lambda)^3}\right]\mathrm{d}k. \qquad (68)$$

The total rate of diffusion is then from (43) equal to

$$\frac{\partial\sigma^2}{\partial T} = A(T)$$

$$\times \int_0^\infty E(k)\left[\frac{2}{3}+\exp(-k^2\sigma^2)\frac{\sin(kU\Lambda)-(kU\Lambda)\cos(kU\Lambda)-(kU\Lambda)^2\,\mathrm{Si}(kU\Lambda)}{(kU\Lambda)^3}\right]\mathrm{d}k, \qquad (69)$$

where $A(T) = A_{22}(T) = A_{33}(T)$.

Equation (69) provides additional information about when the point-source model given by (53) is valid. If σ is large, the high-pass filter in (69) has a cut-off at $k \approx 1/\sigma$.

However, if the sampling time is large and σ is small, the cut-off is at $k \approx 5/U\Lambda$. Equation (69) will therefore reduce to (53) roughly when $\sigma < U\Lambda/5$. For a given sampling time, then, (53) is valid out to the travel time (or downstream distance) at which $\sigma \approx U\Lambda/5$.

Quantitative estimates of σ can be obtained from (69) once functional forms of $A(T)$ and the energy spectrum $E(k)$ are provided. For simplicity, it is assumed here that T is small enough that $A(T) = 2T$. Only the small and intermediate ranges of travel times will thus be considered. This is not a major limitation, however, because the sampling time has little effect in the far-field diffusion limit.

To derive a simple expression for the energy spectrum, it is first assumed that the one-dimensional longitudinal spectrum $F_{11}^E(k_1)$ is of the form

$$F_{11}^E(k_1) = \frac{a}{(1 + bk_1)^{\frac{5}{3}}}, \tag{70}$$

where a and b are parameters that must be determined. This functional form closely resembles measured turbulence spectra in the neutral atmosphere (e.g. Højstrup 1982; Panofsky & Dutton 1984). As is shown in the Appendix, this equation can be used in isotropic turbulence to derive the following expression for the energy spectrum $E(k)$:

$$E(k) = \frac{5m^2}{27} \eta \frac{k}{k_0^2} \frac{3 + 11mk/k_0}{(1 + mk/k_0)^{\frac{11}{3}}}. \tag{71}$$

k_0 is the wavenumber at which $E(k)$ reaches its peak, η is the variance of the velocity fluctuations, and m is a constant equal to $3(7 + 2(26)^{\frac{1}{2}})/55$. With this definition of $E(k)$ and $A(T) = 2T$, the solutions to (69) can be expressed as functions of the dimensionless variables $\eta^{\frac{1}{2}}k_0 T$, γk_0, and $k_0 U\Lambda$. Since $\eta^{\frac{1}{2}}k_0$ is inversely proportional to the Lagrangian timescale of the turbulence, the small and intermediate ranges of travel times are represented by values of $\eta^{\frac{1}{2}}k_0 T$ that are less than unity.

Figure 3 shows numerical solutions of (69) when $E(k)$ is given by (71) and $\gamma k_0 = 0.01$. Three sampling times $k_0 U\Lambda$ are plotted, representing relative diffusion ($k_0 U\Lambda = 0.001$), absolute diffusion ($= 1000$) and an intermediate sampling time ($= 1$). For the most part, the top two curves both grow linearly with the travel time. The relative-diffusion curve has an accelerated growth rate for travel times in the range $0.05 \leqslant \eta^{\frac{1}{2}}k_0 T \leqslant 0.5$; this represents the intermediate range of travel times.

Figure 4(a) shows the variability of σ with the sampling time when the dimensionless travel time $\eta^{\frac{1}{2}}k_0 T$ is fixed at 0.1. Three different curves are shown, representing three values of the dimensionless source size γk_0. As is expected, the sampling time has a greater effect on the diffusion when the source is small.

Little difference exists between the two curves in figure 4(a) representing dimensionless source sizes of 0.01 and 0.001. For both curves, the value of σ in the relative-diffusion limit is about 50% of the value in the absolute-diffusion limit. This ratio of the relative to absolute diffusion only applies to $\eta^{\frac{1}{2}}k_0 T = 0.1$, however. At other travel times, this ratio can fall as low as 20% when the dimensionless source size is 0.001. Values of this ratio in the 20–50% range are in good agreement with other relative-diffusion models and with field measurements (e.g. Smith & Hay 1961; Sawford 1982; Pasquill & Smith 1983; Mikkelsen *et al.* 1987) at small travel times.

The curves in figure 4(a) can also be interpreted as the variation of the time-average diffusion with the flow speed U. A percentage change in U has the same effect on the time-average diffusion as an equivalent percentage change in the sampling time Λ. This
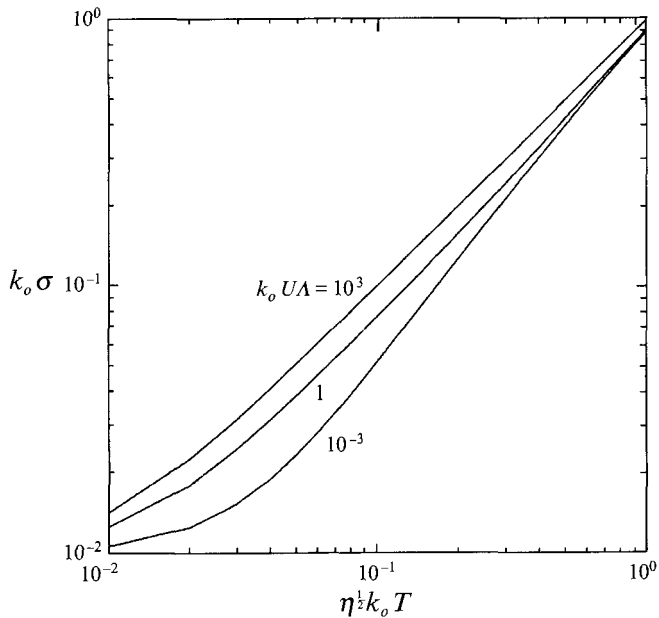
FIGURE 3. Numerical solutions of the sampling-time model as a function of the travel time for three different values of $k_0 UA$. The source size for all three curves is $\gamma k_0 = 0.01$.

variation of the time-average diffusion with the flow speed does not appear in Ogura's (1957) theory because of the single-particle nature of the sampling procedure.

The most rapid sampling-time variations in figure 4(a) occur when $k_0 UA \approx 1$. Because of the influence of the flow speed, this range of rapid variation should occur at fairly small sampling times in typical atmospheric conditions. If $k_0 = 0.003$ m^{-1} and $U = 5$ m s^{-1}, for example, the point $k_0 UA = 1$ is reached when $A \approx 1$ min. The relative-diffusion limit (approximately $k_0 UA < 0.1$) is valid in this example when $A < 7$ s, whereas the absolute-diffusion limit (approximately $k_0 UA > 10$) is valid for $A > 10$ min.

Power laws corresponding to $A^{\frac{1}{5}}$ and $A^{\frac{1}{3}}$ are compared with the sampling-time model in figure 4(b). The $\frac{1}{3}$ power law was derived by dimensional arguments in §4.2, and represents the maximum rate of variation when a large inertial subrange exists. Figure 4(b) indicates that this maximum rate may not generally be reached, as a result of both the limited extent of observed inertial subranges and the effects of the finite source size γ. The $\frac{1}{5}$ power law has been obtained empirically from measurements (Pasquill & Smith 1983; Wollenweber & Panofsky 1989). It seems to fit the model curve in figure 4(b) fairly well in the vicinity of the point $k_0 UA = 1$. However, the model curve corresponds only to a dimensionless source size of 0.001 and a dimensionless travel time of 0.1, and the $\frac{1}{5}$ power law does not fit as well at other source sizes and travel times.

The spectral model given by (71) is intended to describe only the contributions of three-dimensional turbulent eddies. Spectral measurements in the atmosphere indicate that a considerable amount of energy is also associated with quasi two-dimensional motions that have lengthscales much larger than the three-dimensional turbulent eddies (e.g. Smedman-Högström & Högström 1975; Gage 1979; Gifford 1988). These two-dimensional motions start to be important at wavenumbers that are below the so-called
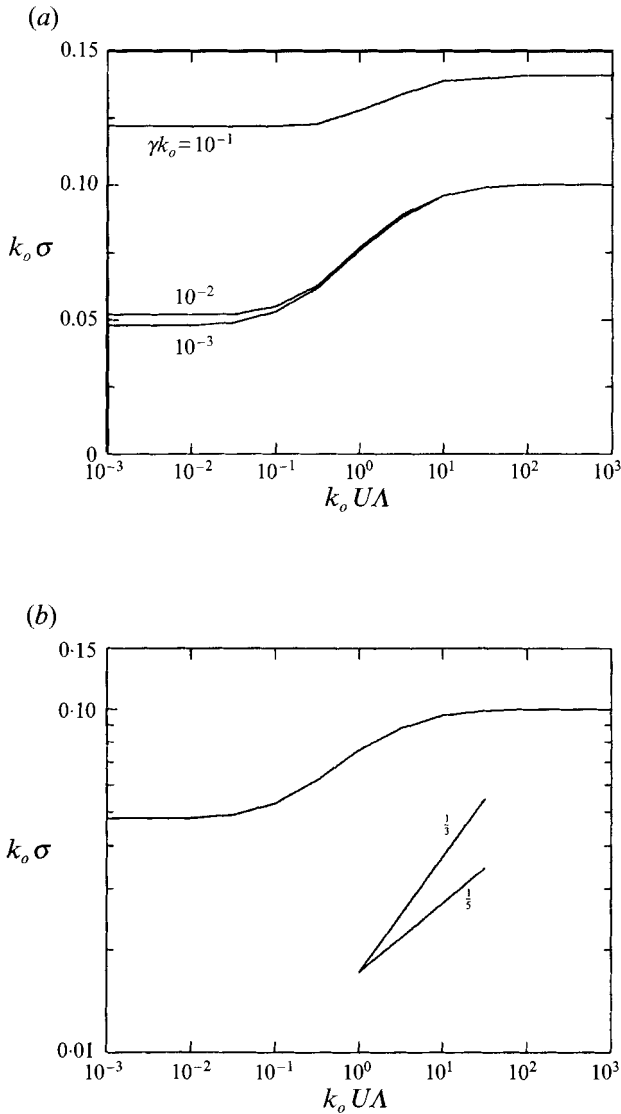
(a)

(b)

FIGURE 4. Numerical solutions of the sampling-time model as a function of the sampling time. (a) shows the solutions for three different values of the source size γk_0. The travel time for all three curves is $\eta^{\frac{2}{3}} k_0 T = 0.1$. (b) compares the model solution at $\gamma k_0 = 0.001$ and $\eta^{\frac{2}{3}} k_0 T = 0.1$ with $\Lambda^{\frac{1}{3}}$ and $\Lambda^{\frac{1}{5}}$ power laws for σ.

spectral gap, which is located at a wavenumber roughly one order of magnitude smaller than the peak wavenumber k_0 of the three-dimensional turbulence.

In regard to figure 4, the presence of these large-scale atmospheric motions indicates that the plateau at $k_0 U\Lambda \geqslant 10$ may only be temporary. If the spectral gap is located at $0.1 k_0$ and the high-pass filter in (69) has a cut-off at $k = 5/U\Lambda$, then these large-scale motions should start to contribute to the time-average diffusion when $k_0 U\Lambda \geqslant 50$. Therefore, the plateau in figure 4 may only be a temporary lull over the range $10 \leqslant k_0 U\Lambda \leqslant 50$. Beyond $k_0 U\Lambda = 50$, the large-scale motions would produce a continued widening of the plume with the sampling time, as has been observed by Hino (1968).

5.3. *Comparisons with diffusion measurements*

In this section, the model derived in §5.2 is compared with diffusion measurements taken both in a wind tunnel and in the field. For these comparisons, $\frac{1}{2}\Sigma_{22}$ is assumed to represent the horizontal variance σ_y^2 of the plume distribution, and $\frac{1}{2}\Sigma_{33}$ is assumed to represent the vertical variance σ_z^2. Likewise, η_{22} and η_{33} are assumed to represent the horizontal cross-stream σ_v^2 and vertical σ_w^2 velocity variances. The model estimates σ are equated with σ_z for the wind-tunnel data and with σ_y for the field data.

Since the model was derived using highly idealized assumptions such as isotropic turbulence, it is expected that some deviations will exist between the model and the observations. However, the spectral functions that are used in the model have shapes that are in fair agreement with observed spectra, so the model should at least explain some of the most significant effects of the sampling time on the diffusion.

The first observations to be considered are from the wind-tunnel experiment described by Nappo (1984). In this experiment, oil-fog smoke was released into a wind tunnel with a mean flow speed of 1 m s^{-1}. Turbulence was generated with a square-bar grid that was modified to produce larger turbulent eddies. The smoke plume was photographed from the side using both a $\frac{1}{60}$ s shutter speed and four-minute time exposures. Gifford's (1957, 1980) technique was then used with the photographs to estimate the vertical diffusion σ_z of the plume at various downstream distances.

Given the lengthscale of the turbulence in the wind tunnel, the estimates of σ_z that Nappo (1984) obtained with the four-minute time exposures are representative of absolute diffusion, whereas the estimates obtained from the photographs with $\frac{1}{60}$ s shutter speeds are representative of relative diffusion. These data can therefore be compared with the absolute and relative diffusion estimates produced by the model in §5.2.

To compare the wind-tunnel data with the model, it is necessary to estimate the source size $\sigma_z(T = 0)$, velocity standard deviation σ_w, and wavenumber scale k_0. From the diameter of the tube that released the smoke, $\sigma_z(0)$ is estimated to be 0.6 cm. The decay of the grid-generated turbulence with downstream distance makes it somewhat difficult to estimate σ_w. By averaging σ_w measurements taken at different downstream distances from the source, Eckman (1989) estimated that $\sigma_w = 7$ cm s^{-1} is a representative value. He also estimated that the Eulerian integral lengthscale l_1 for the downstream velocity component is approximately equal to 30 cm. From (A 11) in the Appendix, the wavenumber scale k_0 can then be estimated as 3.3 m^{-1}.

Figure 5 compares Nappo's σ_z measurements with the sampling-time model. The model is in good agreement with the observations, although the relative diffusion is underestimated at the smallest observed travel time. One possible explanation for this underestimation is that some enhanced mixing of the plume occurred near the source as a result of the initial momentum of the smoke leaving the source. At the largest travel times in figure 5, the observations tend to fall somewhat below the model curves. This is probably due to both the streamwise decay of the turbulence and the deviation of the timescale $A_{33}(T)$ from its near-field value of $2T$ at larger travel times. Neither of these effects are accounted for in the model.

The second set of observations to be considered are the field measurements taken during the Borris Field Experiments (BOREX) in Jutland, Denmark. Descriptions of these experiments are found in Mikkelsen (1983), Mikkelsen & Eckman (1985), and Mikkelsen *et al.* (1987). Military smoke pots were used to generate white smoke during BOREX, and the resulting plumes were photographed from a light aircraft. The photogrammetric method described by Eckman & Mikkelsen (1991) was then used to
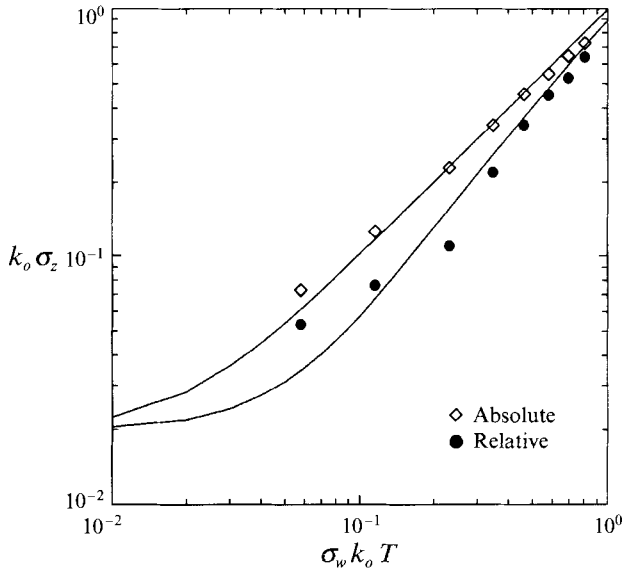
FIGURE 5. Comparison of Nappo's (1984) diffusion data (symbols) with the sampling-time model (solid lines). The upper line is the model absolute diffusion, and the lower line is the model relative diffusion.

estimate the plume's horizontal diffusion σ_y over a range of sampling times extending from 0 (i.e. relative diffusion) to about 30 min.

The two BOREX runs analysed by Eckman (1989) – Run 6 and Run 1B – are used for comparison with the sampling-time model. The measured values of σ_y used here are somewhat different from the values given by Eckman (1989), because the meandering of the plume centreline has been computed using running averages over the available photographs, whereas Eckman (1989) computed the meandering using block averages over the photographs. Running averages were found to provide more consistent results than the block averages when the number of available photographs is small.

Wind speeds and velocity variances for the BOREX runs were measured with sonic anemometers mounted on 10 m towers. These sonic measurements provide the following input values for the diffusion model: $U = 4.7$ m s^{-1} and $\sigma_v = 1.0$ m s^{-1} for Run 6, and $U = 5.9$ m s^{-1} and $\sigma_v = 1.2$ m s^{-1} for Run 1B. The wavenumber scale k_0 was estimated for the runs by using the lateral velocity spectra given by Mikkelsen (1983). Equation (A 9) in the Appendix indicates that within the inertial subrange, k_0 can be estimated as

$$k_0 = \left[\tfrac{9}{4} m^{\frac{2}{3}} \frac{F_{22}(k_1)}{\sigma_v^2} k^{\frac{5}{3}} \right]^{\frac{3}{2}}. \tag{72}$$

From the inertial subrange of Mikkelsen's (1983) spectra, it is estimated that $k_0 = 0.0036$ m^{-1} for Run 6 and 0.0025 m^{-1} for Run 1B.

Figure 6(a) shows the observed and modelled values of σ_y for three different sampling times during Run 6. The model matches the observed variations of σ_y fairly well. Moreover, the model correctly predicts that much of the observed variation of σ_y with the sampling time occurs for sampling times less than about two minutes ($k_0 U \Lambda < 2$), whereas relatively little variation occurs at larger sampling times.

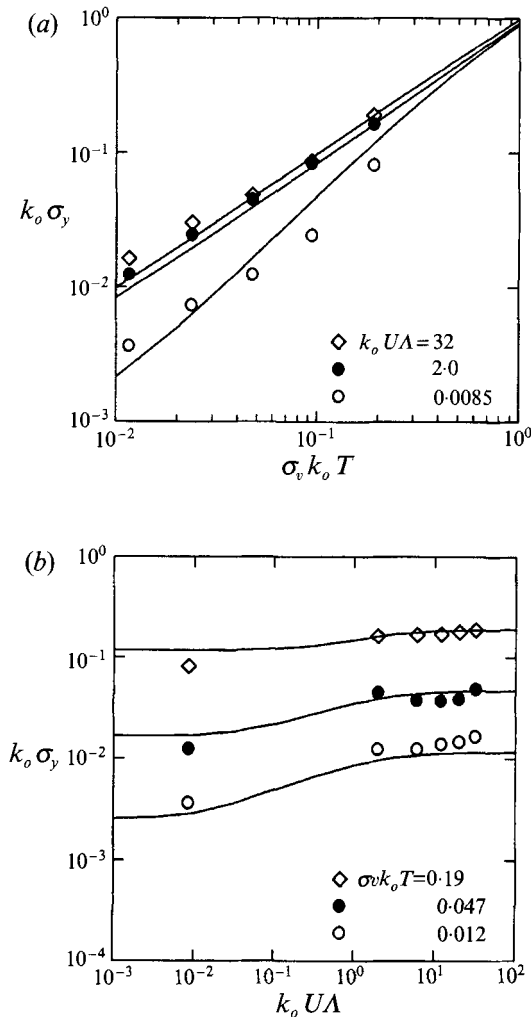In figure 6(b) the Run 6 data and the model are compared at three different travel

FIGURE 6. Comparison of the BOREX Run 6 data (symbols) with the sampling-time model (solid lines). (*a*) shows the data and model at three different sampling times. The model curves are in order of increasing sampling time from the bottom to the top of the plot. (*b*) shows the data and model at three travel times. The model curves are in order of increasing travel time from the bottom to the top of the plot. The relative-diffusion measurements have been placed at $\Lambda = 0.5$ s so that they fit properly on the logarithmic axis.

times. The relative-diffusion measurements in the plot have been assigned a sampling time of 0.5 s so that they fit properly with the logarithmic scaling. As in figure 6(*a*), the model compares favourably with the observed diffusion as a function of both the travel time and the sampling time.

Figure 7 compares the BOREX Run 1B data with the sampling-time model. In both figure 7(*a*) and figure 7(*b*), the model curves compare favourably with the observations. However, the model tends to underestimate the observed relative diffusion at the smallest travel times. This underestimation was also observed in the wind-tunnel data (figure 5). It is not clear whether this underestimation is due to the assumptions inherent in the sampling-time model or to enhanced mixing at the source resulting from the initial momentum or buoyancy of the source.
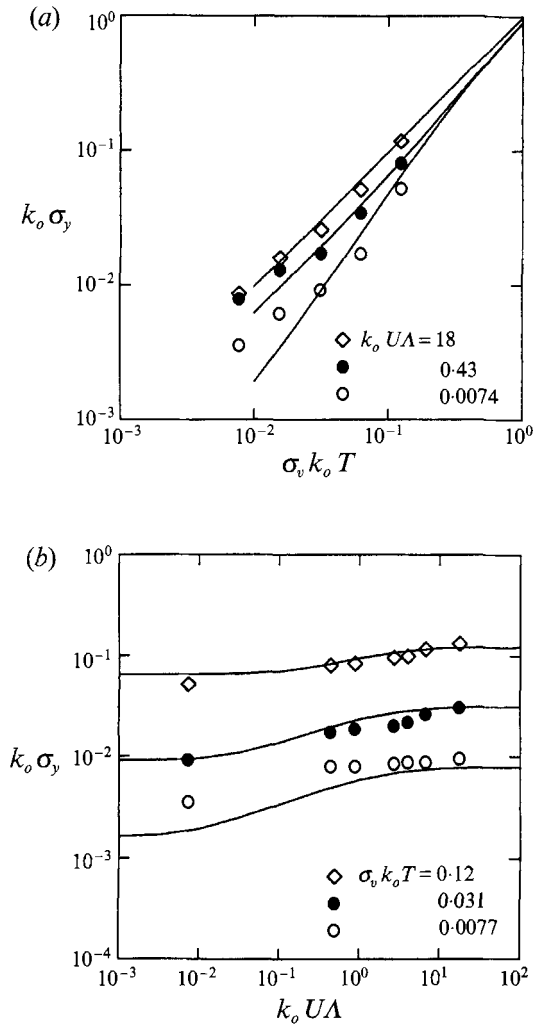
FIGURE 7. Comparison of the BOREX Run 1B data (symbols) with the sampling-time model (solid lines). (*a*) shows the data and model at three different sampling times. The model curves are in order of increasing sampling time from the bottom to the top of the plot. (*b*) shows the data and model at three travel times. The model curves are in order of increasing travel time from the bottom to the top of the plot. The relative-diffusion measurements have been placed at $\Lambda = 0.5$ s so that they fit properly on the logarithmic axis.

6. Conclusions

This paper has considered how turbulent diffusion from a continuous source varies with the sampling time in stationary, homogeneous turbulence. The sampling was assumed to take place at fixed downstream distances from the source. It was shown that this type of sampling is kinematically different from the sampling considered by Ogura (1957), in which the turbulent motions of a single fluid particle are observed over a finite time interval. The sampling effects at fixed downstream distances were shown to depend on two-particle velocity statistics. In contrast, the sampling considered by Ogura depends only on single-particle velocity statistics. Thus, plume sampling at fixed downstream distances is more akin to relative diffusion than to absolute diffusion.

When an extensive inertial subrange exists, the time-average diffusion tensor Σ_{ij} was shown to have three stages of growth that are similar to those for relative diffusion. In the near field, Σ_{ij} is proportional T^2. At intermediate travel times, Σ_{ij} may be proportional to T^3 if the inertial subrange is extensive. In the far field, Σ_{ij} is proportional to T. As the sampling time increases, the near-field range of travel times grows at the expense of the intermediate range. At sufficiently large sampling times, the intermediate range is completely eliminated, and the diffusion reduces to the absolute diffusion described by Taylor's equation.

Dimensional arguments were used to show that when the diffusion is dominated by turbulence in the inertial subrange, Σ_{ij} should be proportional to $\Lambda^{\frac{2}{3}}$, as has been previously obtained by others (e.g. Hino 1968) using spectral arguments. However, the dimensional arguments put additional restrictions on this result, namely, the diffusion must be in the near-field limit, and the initial size of the cloud must be small compared with the length $U\Lambda$. The model results in §5 indicate, however, that the $\Lambda^{\frac{2}{3}}$ power law may not generally be reached in the atmosphere, because of the limited extent of the inertial subrange and the effects of the finite source size.

The simple models developed in §5 were shown to be in fairly good agreement with diffusion observations both in a wind tunnel and in the field. In both the model and the field data, the diffusion varies most rapidly with the sampling time when the sampling time is on the order of one minute. Much less variation is observed for sampling times on the order of ten minutes, although the model does not account for large-scale quasi two-dimensional atmospheric motions that will affect the observed diffusion at sampling times significantly larger than ten minutes.

The models in §5 have important practical implications. For example, the band-pass spectral filtering that is often used as a paradigm for turbulent diffusion was shown not to exist when the sampling takes place at fixed downstream distances from a source. Instead, this band-pass filtering requires the single-particle sampling that is invoked in Ogura's (1957) theory. Hence, care should be taken in using the band-pass filtering as a paradigm for turbulent diffusion.

Another important implication of the models is the effect of the mean flow speed U. Unlike Ogura's equation, these models indicate that the sampling time effects are determined by product $U\Lambda$, and not just by Λ. This means that two sets of diffusion measurements with the same sampling time Λ will not be comparable if the mean flow speed U is different for each set. To account for the speed effects, diffusion data with different sampling times should be compared using the length $U\Lambda$. This has not generally been done in the past.

Appendix

In isotropic turbulence, the energy spectrum $E(k)$ is related to the one-dimensional longitudinal spectrum $F_{11}^E(k_1)$ by the expression (Batchelor 1953)

$$E(k) = k^3 \frac{\mathrm{d}}{\mathrm{d}k}\left[\frac{1}{k}\frac{\mathrm{d}F_{11}^E(k)}{\mathrm{d}k}\right]. \qquad (A\ 1)$$

Given the form of F_{11}^E in (70), $E(k)$ has the form

$$E(k) = \tfrac{5}{9}abk \frac{3+11bk}{(1+bk)^{\frac{11}{3}}}.$$ (A 2)

The wavenumber scale k_0 is defined as the wavenumber at which $E(k)$ has a maximum. It is therefore related to the parameter b through the expression

$$k_0 = \frac{3}{55} \frac{7+2(26)^{\frac{1}{2}}}{b} = \frac{m}{b}.$$ (A 3)

Equation (A 2) can then be written as

$$E(k) = \tfrac{5}{9}am \frac{k}{k_0} \frac{3+11mk/k_0}{(1+mk/k_0)^{\frac{11}{3}}}.$$ (A 4)

An expression for the parameter a can be obtained by requiring that the integral of $E(k)$ over all positive wavenumbers be equal to $\tfrac{3}{2}\eta$, where η is the velocity variance in isotropic turbulence. This gives

$$a = \frac{m}{3} \frac{\eta}{k_0},$$ (A 5)

and

$$E(k) = \frac{5m^2}{27} \eta \frac{k}{k_0^2} \frac{3+11mk/k_0}{(1+mk/k_0)^{\frac{11}{3}}}.$$ (A 6)

Given the above derivations for the parameters a and b, the original longitudinal spectrum can be written as

$$F_{11}^E(k_1) = \frac{m}{3} \frac{\eta}{k_0} \frac{1}{(1+mk_1/k_0)^{\frac{5}{3}}}.$$ (A 7)

Moreover, the lateral spectrum $F_{22}^E(k_1)$ is related to $F_{11}^E(k_1)$ in isotropic turbulence by the equation (Batchelor 1953)

$$F_{22}^E(k_1) = \tfrac{1}{2}\left[F_{11}^E(k_1) - k_1 \frac{\mathrm{d}F_{11}^E}{\mathrm{d}k_1}\right].$$ (A 8)

Hence, the expression for F_{22}^E is

$$F_{22}^E(k_1) = \frac{m}{18} \frac{\eta}{k_0} \frac{3+8mk_1/k_0}{(1+mk_1/k_0)^{\frac{8}{3}}}.$$ (A 9)

Since k_0 represents the peak of the energy spectrum, it should be inversely related to the integral lengthscales of the turbulence. The integral lengthscale l_1 for the longitudinal velocity fluctuations is defined as

$$l_1 = \pi \frac{F_{11}^E(0)}{\eta}.$$ (A 10)

By using (A 7), the scale becomes

$$l_1 = \frac{m\pi}{3k_0}.$$ (A 11)

Likewise, the integral lengthscale l_2 for the lateral velocity fluctuations can be expressed as

$$l_2 = \pi \frac{F_{22}^E(0)}{\eta} = \frac{m\pi}{6k_0}. \tag{A 12}$$

REFERENCES

BATCHELOR, G. K. 1950 The application of the similarity theory of turbulence to atmospheric diffusion. *Q. J. R. Met. Soc.* **76**, 133–146.

BATCHELOR, G. K. 1952 Diffusion in a field of homogeneous turbulence. II. The relative motion of particles. *Proc. Camb. Phil. Soc.* **48**, 345–362.

BATCHELOR, G. K. 1953 *The Theory of Homogeneous Turbulence*. Cambridge University Press.

BATCHELOR, G. K. 1964 Diffusion from sources in a turbulent boundary layer. *Arch. Mech. Stosowanej* **16**, 661–670.

DORAN, J. C., HORST, T. W. & NICKOLA, P. W. 1978 Variations in measured values of lateral diffusion parameters. *J. Appl. Met.* **17**, 825–831.

DURBIN, P. A. 1980 A stochastic model of two-particle dispersion and concentration fluctuations in homogeneous turbulence. *J. Fluid Mech.* **100**, 279–302.

ECKMAN, R. M. 1989 The influence of the sampling time on diffusion measurements in the atmosphere. PhD dissertation, The Pennsylvania State University, University Park.

ECKMAN, R. M. & MIKKELSEN, T. 1991 Estimation of horizontal diffusion from oblique aerial photographs of smoke clouds. *J. Atmos. Oceanic Technol.* **8**, 873–878.

GAGE, K. S. 1979 Evidence for a $k^{-\frac{5}{3}}$ law inertial range in mesoscale two-dimensional turbulence. *J. Atmos. Sci.* **36**, 1950–1954.

GAUTSCHI, W. & CAHILL, J. H. 1964 Exponential integral and related functions. In *Handbook of Mathematical Functions with Formulas, Graphs, and Mathematical Tables* (ed. M. Abramowitz & I. Stegun), p. 227. US National Bureau of Standards.

GEORGOPOULOS, P. G. & SEINFELD, J. H. 1988 Estimation of relative dispersion parameters from atmospheric turbulence spectra. *Atmos. Environ.* **22**, 31–41.

GIFFORD, F. A. 1957 Relative atmospheric diffusion of smoke puffs. *J. Met.* **14**, 410–414.

GIFFORD, F. A. 1980 Smoke as a quantitative atmospheric diffusion tracer. *Atmos. Environ.* **14**, 1119–1121.

GIFFORD, F. A. 1988 A similarity theory of the tropospheric turbulence energy spectrum. *J. Atmos. Sci.* **45**, 1370–1379.

HANNA, S. R., BRIGGS, G. A. & HOSKER, R. P. 1982 Handbook on atmospheric diffusion. DOE/TIC-11223, Technical Information Center, US Dept of Energy.

HAY, J. S. & PASQUILL, F. 1959 Diffusion from a continuous source in relation to the spectrum and scale of turbulence. *Adv. Geophys.* **6**, 345–365.

HINO, M. 1968 Maximum ground-level concentration and sampling time. *Atmos. Environ.* **2**, 149–165.

HØJSTRUP, J. 1982 Velocity spectra in the unstable boundary layer. *J. Atmos. Sci.* **39**, 2239–2248.

KRISTENSEN, L., JENSEN, N. O. & PETERSEN, E. L. 1981 Lateral dispersion of pollutants in a very stable atmosphere – the effect of meandering. *Atmos. Environ.* **15**, 837–844.

MIKKELSEN, T. 1983 The Borris field experiment: observations of smoke diffusion in the surface layer over homogeneous terrain. Risø-R-479, Risø National Laboratory, Denmark.

MIKKELSEN, T. & ECKMAN, R. M. 1985 Instantaneous observations of plume dispersion in the surface layer. In *Air Pollution Modeling and It Application IV* (ed. C. De Wispelaere), p. 549. Plenum.

MIKKELSEN, T., LARSEN, S. E. & PÉCSELI, H. L. 1987 Diffusion of Gaussian puffs. *Q. J. R. Met. Soc.* **113**, 81–105.

MONIN, A. S. & YAGLOM, A. M. 1971 *Statistical Fluid Mechanics: Mechanics of Turbulence*, vol. 1. MIT Press.

MONIN, A. S. & YAGLOM, A. M. 1975 *Statistical Fluid Mechanics: Mechanics of Turbulence*, vol. 2. MIT Press.

NAPPO, C. J. 1984 Turbulence and dispersion parameters derived from smoke-plume photoanalysis. *Atmos. Environ.* **18**, 299–306.

OGURA, Y. 1957 The influence of finite observation intervals on the measurement of turbulent diffusion parameters. *J. Met.* **14**, 176–181.

OGURA, Y. 1959 Diffusion from a continuous source in relation to a finite observation interval. *Adv. Geophys.* **6**, 149–159.

PANOFSKY, H. A. & DUTTON, J. A. 1984 *Atmospheric Turbulence: Models and Methods for Engineering Applications.* John Wiley.

PASQUILL, F. & SMITH, F. B. 1983 *Atmospheric Diffusion.* Halsted Press.

RICHARDSON, L. F. 1926 Atmospheric diffusion shown on a distance-neighbor graph. *Proc. R. Soc. Lond.* **110**, 709–737.

SAWFORD, B. L. 1982 Comparison of some different approximations in the statistical theory of relative dispersion. *Q. J. R. Met. Soc.* **108**, 191–206.

SHEIH, C. M. 1980 On lateral dispersion coefficients as functions of averaging time. *J. Appl. Met.* **19**, 557–561.

SHIMANUKI, A. 1961 Diffusion from the continuous source with finite release time. *Sci. Rep. Tôhoku Univ.* (5) **12**, 184–190.

SMEDMAN-HÖGSTRÖM, A. & HÖGSTRÖM, U. 1975 Spectral gap in surface-layer measurements. *J. Atmos. Sci.* **32**, 340–350.

SMITH, F. B. & HAY, J. S. 1961 The expansion of clusters of particles in the atmosphere. *Q. J. R. Met. Soc.* **87**, 82–101.

SUTTON, O. G. 1953 *Micrometeorology.* McGraw-Hill.

TAYLOR, G. I. 1921 Diffusion by continuous movements. *Proc. Lond. Math. Soc.* (2) **20**, 196–212.

THOMSON, D. J. 1987 Criteria for the selection of stochastic models of particle trajectories in turbulent flows. *J. Fluid Mech.* **180**, 529–556.

THOMSON, D. J. 1990 A stochastic model for the motion of particle pairs in isotropic high Reynolds number turbulence, and its application to the problem of concentration variance. *J. Fluid Mech.* **210**, 113–153.

WOLLENWEBER, G. C. & PANOFSKY, H. A. 1989 Dependence of velocity variance on sampling time. *Boundary-Layer Met.* **47**, 205–215.